Nonequilibrium Chromosome Looping via Molecular Slip Links

C. A. Brackley,[1] J. Johnson,[1] D. Michieletto,[1] A. N. Morozov,[1] M. Nicodemi,[2] P. R. Cook,[3] and D. Marenduzzo[1]
[1]SUPA, School of Physics and Astronomy, University of Edinburgh, Peter Guthrie Tait Road, Edinburgh EH9 3FD, United Kingdom
[2]Dipartimento di Fisica, Universita' di Napoli Federico II, INFN Napoli, CNR, SPIN, Complesso Universitario di Monte Sant'Angelo, 80126 Naples, Italy
[3]Sir William Dunn School of Pathology, University of Oxford, South Parks Road, Oxford OX1 3RE, United Kingdom
(Received 11 April 2017; published 26 September 2017)

We propose a model for the formation of chromatin loops based on the diffusive sliding of molecular slip links. These mimic the behavior of molecules like cohesin, which, along with the CTCF protein, stabilize loops which contribute to organizing the genome. By combining 3D Brownian dynamics simulations and 1D exactly solvable nonequilibrium models, we show that diffusive sliding is sufficient to account for the strong bias in favor of convergent CTCF-mediated chromosome loops observed experimentally. We also find that the diffusive motion of multiple slip links along chromatin is rectified by an intriguing ratchet effect that arises if slip links bind to the chromatin at a preferred "loading site." This emergent collective behavior favors the extrusion of loops which are much larger than the ones formed by single slip links.

DOI: 10.1103/PhysRevLett.119.138101

Introduction.—The formation of long-range contacts, or loops, within DNA and chromosomes critically affects gene expression [1,2]. For instance, looping between specific regulatory elements, such as enhancers and promoters, can strongly increase transcription rates in eukaryotes [1]. The formation of these loops can often be successfully predicted by equilibrium polymer physics models, which balance the energetic gain of protein-mediated interactions with the entropic loss of looping [3–5].

However, recent high-throughput chromosome conformation capture ("Hi-C") experiments [6,7] have fundamentally challenged the view that equilibrium physics is sufficient to model chromosome looping. These experiments showed that the genomes of most eukaryotic organisms are partitioned into domains, many of which are enclosed within a chromosome loop, 100–1000 kilobasepairs (kpb) in size. The bases of these loops tend to be enriched in binding sites for the CCCTC-binding factor (CTCF) [7,8]. The DNA-binding motif of CTCF is not palindromic, so it has a specific direction along DNA. Surprisingly, Hi-C analyses revealed that most of the CTCF binding sequences only form a loop if they are in a "convergent" orientation [Fig. 1(a)] [7,9]. Very few contacting CTCFs have a "parallel" orientation, and virtually none a "divergent" one. This strong bias is puzzling, because, if we imagine drawing arrows on the chromatin fiber (corresponding to CTCF directionality), then two loops with a pair of convergent or divergent arrows at their base have the same 3D structure [7,10]; hence, they would be equally likely according to equilibrium polymer models. Here we propose a nonequilibrium model that can account for this bias.

In most cases CTCF-mediated loops are associated with cohesin [13], a ringlike protein complex thought to bind DNA by topologically embracing it [14]. There are two models for how cohesin might achieve this—as a dimer acting as a pair of molecular "handcuffs" in which each ring embraces one DNA duplex [Fig. 1(a)], or as a single ring that embraces two duplexes [15]. In both cases, the dimer or ring acts as a sliding bridge or molecular slip link [16,17]. Experiments show that cohesin topologically links to DNA (with binding mediated by "loader proteins" [13,18]), can slide along DNA or chromatin diffusively, and remains bound for $\tau \sim 20$ min before dissociating (a process mediated by "unloader proteins") [18–23].

One recent attempt to address the mechanism underlying CTCF-mediated looping is the "loop extrusion model" which argues that cohesin (or other "loop extruding factors") can create loops of 100–1000 kbp by actively traveling in opposite directions along the chromosome [24–26]. This model is appealing as it naturally explains the bias in favor of convergent loops, if cohesin gets stuck when it finds a CTCF binding site pointing towards it (but passes over CTCF otherwise). However, the model is based on some assumptions lacking experimental evidence: it requires (i) that each cohesin can determine and maintain the correct direction in order to extrude (rather than shrink) a loop, and (ii) that cohesin must extrude loops at a speed of $v \sim 5$ kbp/ min, which is faster than that of RNA polymerase. While cohesin is known to have ATPase activity, this is not thought to be involved in directional motion; rather, it drives the gate-opening mechanism needed to link to DNA [13].

Here, we propose an alternative model for the formation of CTCF-mediated loops, which does not require unidirectional motion, nor any energetically costly explicit bias favoring loop extrusion. We start from the observation that the molecular topology of cohesin—that of a slip link—is compatible with diffusive sliding along chromatin [19]. From this premise, we formulate a nonequilibrium model

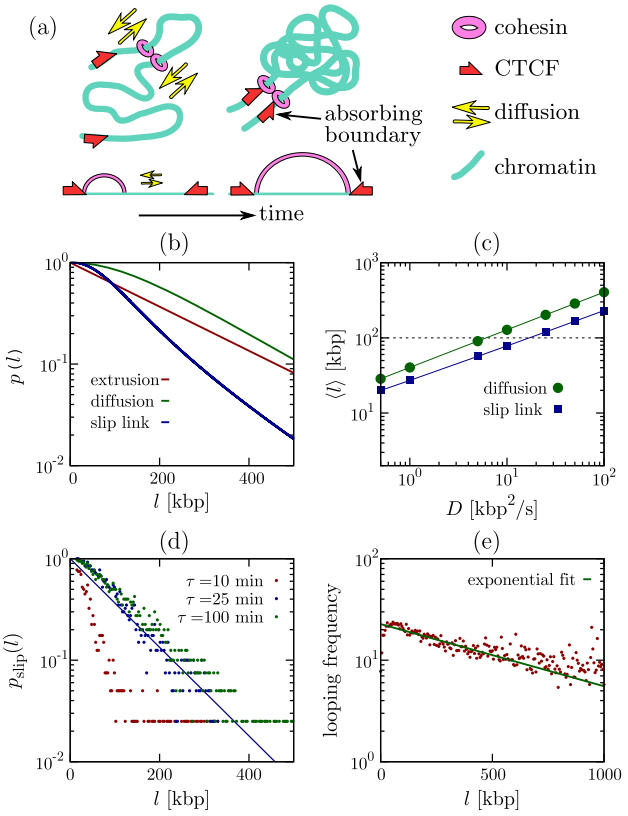

FIG. 1. Nonequilibrium chromosome looping. (a) Schematic of our model of diffusing slip links. (b) Probability of nonequilibrium loop formation in exactly solvable 1D models as a function of loop size l. Curves correspond to models involving (i) extrusion, (ii) diffusion, and (iii) slip links. Parameters are $k_{\rm off}^{-1} =$ 20 min and (i) $v = 10$ kbp/min; (ii), (iii) $D = 25$ kbp^2/s; (iii) $\sigma_{\rm sl} = 1$ kbp, and $c = 1$ [11]. (c) Average loop size for models involving diffusion and slip links. Parameters are as in (b), apart from D which is varied. (d) Nonequilibrium looping probability for a slip link, computed from BD simulations, with different $k_{\rm off}^{-1} = \tau$. The blue line shows an exponential fit for $k_{\rm off}^{-1} = 25$ min. (e) Analysis of ChIA-PET experiments for CTCF contacts within a Mbp [12] (log-linear plot).

where the binding and unbinding kinetics of cohesin violates detailed balance, modeling the fact that both its loading and unloading onto chromatin requires ATP [13,27]. We show that within this nonequilibrium context passive sliding is sufficient to account for both the creation of loops of hundreds of kbp before dissociation, and the bias favoring convergent CTCF binding. We further show that many-body interactions between diffusing slip links which bind close to a preferred "loading site" lead to the emergence of an "osmotic ratchet" promoting loop extrusion over shrinking, again in the absence of any bias in the microscopic molecular diffusion.

Single slip links.—We begin by discussing an exactly solvable 1D model where a slip link consisting of two cohesin rings in a dimer slides along the chromatin fiber. We assume that this binds with the cohesin rings at adjacent positions on the fiber (as in [25]), and that there is a constant detachment rate $k_{\rm off} = \tau^{-1}$. Data suggest that cohesin interacts with CTCF in a directional manner [10,25,28], so we assume that slip links bind to CTCF sites which face them, and are reflected off those which do not; further we assume that when the slip link reaches the two convergent CTCF sites it undergoes a conformational change decreasing $k_{\rm off}$. We consider two CTCF proteins bound to the fiber at a separation l in a convergent orientation. [The case of a divergent pair is treated in [29], and as expected leads to no stable looping (Fig. S1 [29]).] For simplicity, we allow the rings forming one cohesin to diffuse until their separation reaches l, or until the dimer spontaneously unbinds, and consider both to be absorbing states. This is a nonequilibrium model as the binding-unbinding kinetics violate detailed balance, in line with experimental evidence that ATP is required for both [13,27].

At time t, the slip link holds together a chromatin loop of size $x(t)$. In order to take into account the entropic loss associated with this loop, we include an effective thermodynamic potential $V(x)$ (detailed below). The probability that the cohesin holds a loop of size x at time t, obeys the following generalized Fokker-Plank equation:

$$\frac{\partial p(x,t)}{\partial t} = -k_{\rm off} p(x,t) + \frac{\partial}{\partial x}\left(\frac{1}{\gamma}\frac{dV}{dx} p(x,t)\right) + D\frac{\partial^2}{\partial x^2} p(x,t), \tag{1}$$

where D and γ are the effective diffusion and drag coefficients describing the relative motion between chromatin and cohesin. The fluctuation-dissipation theorem implies $D = k_B T/\gamma$. The initial condition for Eq. (1) is $p(x,0) = \delta(x - \sigma_{\rm sl})$, where $\sigma_{\rm sl}$ is the size of the slip link. Boundary conditions are reflecting at $x = \sigma_{\rm sl}$ and, for simplicity, absorbing at $x = l$—replacing the latter with an attractive interaction between CTCF and cohesin does not affect our results (Fig. S1 [29]).

We consider three possible cases. First, we model "loop extrusion" as in [24,25,40] by setting $D = 0$ and $(1/\gamma)(dV/dx) = -v$, with v the extrusion speed. Second, we consider a "diffusion" model where cohesin diffuses in the absence of a potential, $V = 0$. Third, we consider a cohesin dimer diffusing in a potential $V(x) = ck_BT\log(x)$, which models the entropic cost of looping via the known contact probability $p_{\rm eq}(x) \sim x^{-c}$. Here c is a universal exponent: in 3D, $c = 1.5$ for random walk loops [41], $c \sim 2.1$ for internal looping within self-avoiding chains [41,42], and $c = 1$ for contacts within a "fractal globule" [11]. We refer to the case with a logarithmic potential as the "slip link" model, as it most closely resembles the dynamics of slip links on polymers [4,16,17].

As detailed in [29], we can analytically find the probability that a cohesin dimer binding at $t = 0$ will, at some point, form a CTCF-mediated loop before detaching.

Denoting this probability by $p(l)$, the three models predict the following dependence on loop size l [Fig. 1(b)]:

$$p_{\mathrm{extr}}(l) = e^{-k_{\mathrm{off}} l/v}; \qquad p_{\mathrm{diff}}(l) = \frac{1}{\cosh(\alpha l)},$$
$$p_{\mathrm{slip}}(l) = \left(\frac{l}{\sigma_{\mathrm{sl}}}\right)^{n} \frac{I_{m-1}(\alpha l)K_m(\alpha l) + I_m(\alpha l)K_{m-1}(\alpha l)}{I_{m-1}(\alpha\sigma_{\mathrm{sl}})K_m(\alpha l) + I_m(\alpha l)K_{m-1}(\alpha\sigma_{\mathrm{sl}})}, \tag{2}$$

where $\alpha = \sqrt{k_{\mathrm{off}}/D}$, $n = (1-c)/2$, and $m = (1+c)/2$; I and K denote the modified Bessel functions of the first and second kind, respectively. Note that we have taken the $\sigma_{\mathrm{sl}} \to 0$ limit for the loop extrusion [$p_{\mathrm{extr}}(l)$] and diffusion [$p_{\mathrm{diff}}(l)$] cases.

For large l, Eqs. (2) predict exponential decay of CTCF-mediated looping probabilities for all cases [Fig. 1(b)], with a power law correction for slip links, $p_{\mathrm{slip}}(l) \sim e^{-\alpha l} l^{-c/2}$. This is markedly different from the power laws determining the looping probability of an equilibrium polymer [16,17]. The decay length is v/k_{off} for the loop extrusion model [25], and $\alpha^{-1} = \sqrt{D/k_{\mathrm{off}}}$ for the diffusion and slip link models; these are therefore the typical looping lengths formed before cohesin detaches. CTCF-mediated loop lengths *in vivo* are typically ~100 kbp [7,10]; taking $\tau = 20$ min means loop extrusion is viable if $v > 5$ kbp/min, whereas the diffusion or slip link models require $D > 10$ kbp^2/s [Fig. 1(c); see Conclusions and [29] for a discussion of the likely *in vivo* value of D].

Our 1D theory does not account for the motion of the chromatin fiber, or for the coupling between instantaneous polymer conformation in 3D and slip link diffusivity; to account for these aspects, we also present results from 3D Brownian dynamics (BD) simulations [29]. We modeled a chromatin fiber as a bead-and-spring polymer with bead diameter $\sigma = 30$ nm, compaction $C = 100$ bp/nm, and persistence length $l_p = 4\sigma$ [43]; cohesin slip links were modeled by two rigid rings (each with diameter $2R \sim 3.5\sigma$, and thickness $\sigma_{\mathrm{sl}} = \sigma$, while $D \sim 5$ kbp^2/s [29]). Each ring embraces the fiber, and the two rings are linked via a semiflexible hinge, favoring a planar handcuff configuration with the center of the rings a distance $2R$ apart (Fig. S5 [29]). Figure 1(d) shows the *nonequilibrium* looping probability $p_{\mathrm{slip}}(l)$ for different values of k_{off} found in these 3D simulations. The results confirm our 1D model predictions that large loops can form via diffusive sliding—e.g., a 100 kbp loop forms with probability ~0.3 if $k_{\mathrm{off}}^{-1} = \tau = 25$ min (see also [29], Figs. S7, S8, and Movie 1). As in the 1D models, the decay of $p_{\mathrm{slip}}(l)$ is exponential [Fig. 1(d)].

Hi-C experiments measuring the frequency of contacts between all genomic loci largely support a power law decay of contact probability [44]. However, that analysis does not distinguish between CTCF-mediated loops and other contacts [43–46]. Chromatin interaction analysis by paired-end tag sequencing (ChIA-PET) experiments [10] are able to single out contacts where both anchor points are bound to a protein of interest. Intriguingly, in CTCF ChIA-PET data [12], fitting to an exponential leads to reasonable decay lengths (loop size) of ~500–1000 kbp [Fig. 1(e)], whereas fitting to a power law yields an effective exponent which is far from those expected from equilibrium polymer physics [Fig. S11(a) [29]].

Multiple slip links and the osmotic ratchet.—So far, we have considered a single slip link. When multiple slip links coexist on the same chromatin segment, they may interact either sterically or entropically. To quantify how this affects loop formation, we performed simple 1D simulations capturing the stochastic dynamics of each side (monomer) of N slip links which interact solely via excluded volume, and diffuse along a chromatin fiber of size L discretized into segments of length σ_{sl} [Figs. 2(a)–2(c), and [29]]. Each slip link can exist in an unbound or chromatin-bound state with binding and unbinding rates k_{on} and k_{off}, respectively. When binding, the two slip link monomers always occupy neighboring sites along the fiber. In [29], we present a model which also includes a "looping weight" (Figs. S3 and S4), accounting for the entropy of a loop network [16,17]. This effective potential has a quantitative effect but does not modify the qualitative trends; hence, we report here results from the simpler case without the weight.

We consider two cases: (i) with slip links binding at random (unoccupied) locations on the fiber, and (ii) with binding occurring at a preferred "loading site." Figure 2(a) shows the time average of the maximal loop size $\langle l_{\mathrm{max}} \rangle$ in a steady state as a function of N for the first case. As the fiber gets more crowded, the slip links form consecutive loops [Fig. 2(a), inset, and Fig. S3(c)] competing with each other. Consequently, $\langle l_{\mathrm{max}} \rangle$ decreases steadily with N [Fig. 2(a)].

A strikingly different result is found when slip links always bind at the same location. This scenario mimics the experimental finding that linking of cohesin to DNA is facilitated by a loader protein (e.g., Scc2 or NIPBL), which has preferential binding sites within the genome [1,18,23]. In this case, we observe that the maximum loop size *increases* with N [Fig. 2(b)], favoring loop growth over shrinking. Therefore, the system now works as a ratchet, rectifying the diffusion of the two ends of the loop subtended by a slip link. The typical loop network found in a steady state is different from the case of random rebinding, and entails a significant proportion of nested loops [6 out of 11 in Fig. 2(b), inset, and Fig. S3(d)], which reinforce each other. Figure 2(c) shows the probability distribution of sizes for the largest loop and confirms the dramatic difference between the cases with and without loading. We also performed BD simulations of a chromatin fiber interacting with N slip links which can bind and unbind, with a loading site [29]. These 3D simulations confirm the ratchet effect, and show that the outer loops can easily span hundreds of kbp [Fig. 2(d); Fig. S8 [29]] even with as few as $N = 3$ slip links. This ratchet effect may provide a microscopic basis for the loop extrusion model in

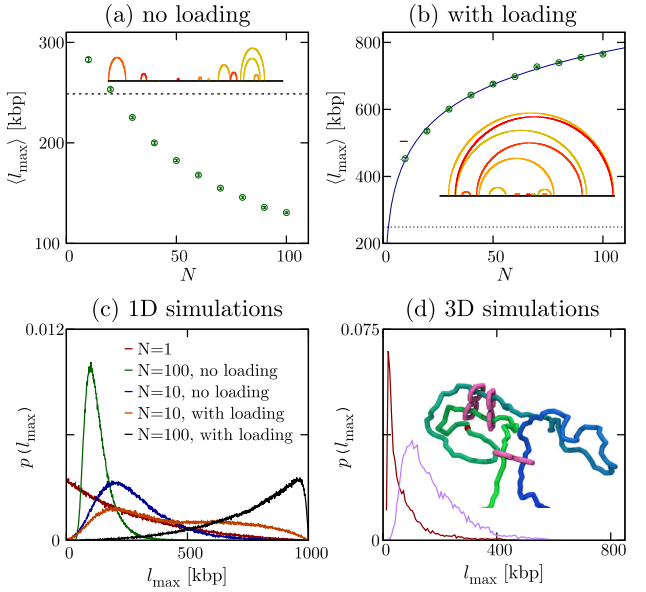

FIG. 2. Multiple slip links and the osmotic ratchet. (a),(b) Results from 1D simulations of diffusing slip links rebinding either (a) randomly, or (b) at a loading site. Plots show the time average of the largest loop (for the case with looping weight see [29], Fig. S4). Parameters are $\sigma_{sl} = 1$ kbp, $L = 1000$ kbp, $k_{on}^{-1} = k_{off}^{-1} = 25$ min, the diffusion coefficient of a monomer is $D \sim 33.35$ kbp^2/s, while N is varied. There are reflecting boundary conditions at the two ends of the fiber. Typical configurations for $N = 20$ are shown as insets, as "looping diagrams" showing the loop network [29]. The dotted line in (a),(b) denotes the average loop size with a single slip link; the solid line in (b) is a fit to $a + b \log N$ (see text). (c) Probability distribution of the largest loop size for different N with or without loading (for the case with looping weight see [29], Fig. S4). (d) Results from 3D BD simulations of multiple slip links with loading, for $L = 3000$ kbp, $k_{off}^{-1} = 25$ min. The plots show the probability distribution of the size of the largest loop for $N = 1$ (with $k_{on} \to \infty$), and $N = 3$ (with $k_{on} = 10 k_{off}$, snapshot shown as an inset).

[24–26], valid under conditions where several cohesins (or other slip links) are bound to the same chromatin region.

While the simulations discussed thus far were done in dilute conditions, simulations of slip links moving on chromatin fibers at physiological concentrations reach qualitatively similar conclusions (Fig. S9 [29]). The chromatin contact patterns arising from 1D or 3D simulations are also reminiscent of intra-TAD contact maps observed by Hi-C (Figs. S9, S10 [29]), although *in vivo* we expect other mechanisms besides cohesin-mediated looping to contribute to contact formation [43,44,46].

To understand the emergence of a self-organized ratchet, we construct a simple theory by analyzing the 1D model without looping weight (see [29] for more details). The key factor is the existence of a nonuniform slip link density $\rho(x)$, and hence an osmotic pressure; the associated gradient creates a force that rectifies the motion of cohesin rings placed close to the loading site. If volume exclusion does not significantly affect the density and pressure profiles (an assumption which holds in our 1D stochastic simulations, Fig. S2 [47]), we can write down the following phenomenological equation determining the size of a loop, l, subtended by a symmetrically progressing slip link starting from the loader:

$$\frac{dl}{dt} = -2D\sigma_{sl}\left[\frac{\partial\rho}{\partial x}\right]_{x=l/2} = k_{on}N_{off}\sigma_{sl}e^{-\alpha l/2}, \qquad (3)$$

where $N_{off} = Nk_{off}/(k_{on} + k_{off})$ is the average number of unbound cohesins. The maximal speed of this "osmotic ratchet" is achieved for loops close to the loading site. Equation (3) predicts that at a given time, l should grow logarithmically with N, and our data are indeed fitted well by the functional form $a + b \log N$ [Fig. 2(b)].

Conclusions.—In summary, we proposed a dynamical model through which molecular slip links might organize chromosomal loops. First, we showed that diffusive sliding of cohesin [18,48,49] naturally explains the experimentally observed bias favoring convergent over divergent CTCF loops. Second, the probability of formation of cohesin/CTCF-mediated loops does not obey a power law, in stark contrast with the case of polymer loops in thermodynamic equilibrium. Finally, we found that when multiple slip links bind to chromatin at a "loading site" rather than randomly, a ratchet effect arises, which favors the formation of much larger loops than are possible with single slip links. Each of these results critically depends on our assumption that the cohesin binding kinetics violate detailed balance, which is motivated by the fact that its loading and unloading requires ATP.

An important consequence of our work is that it predicts which values of the 1D diffusion coefficient, D_0 (in μm^2/s) and chromatin compaction, C (in bp/nm), are needed for slip links to form CTCF-mediated loops of hundreds of kbp, as found in mammalian genomes [7]. For a single slip link, we need $D = D_0C^2 > 10$ kbp^2/s; for multiple slip links due to the ratchet effect a substantially smaller D suffices. The worst-case scenario occurs for the least compact structure, a 10-nm chromatin fiber with $C \sim 20$ bp/nm: this requires $D_0 > 0.025$ μm^2/s. Recent experiments in *Xenopus* egg extracts [49] found $D_0 = 0.2525 \pm 0.0031$ μm^2/s for acetylated cohesin on chromatin [49], comfortably fulfilling the requirement (see [29] for a more quantitative discussion of these and other experiments). Those experiments were performed on a stretched fiber, whereas *in vivo* cohesin dimers are associated with folded chromatin and need to work in a crowded nucleoplasm. Our BD simulations suggest that long enough loops can still be formed when these aspects are taken into account. We hope that our work will prompt new studies to measure diffusion of multiple cohesins on reconstituted chromatin fibers. Particularly our model shows that an extrusion mechanism could arise without the previously

proposed motor activity, and it is important that future experiments are designed to discriminate between these models.

Research outputs generated through the EPSRC Grant No. EP/I004262/1 can be found at [50].

This work was supported by ERC (CoG 648050, THREEDCELLPHYSICS), by ISCRA Grants No. HP10CYFPS5 and HP10CRTY8P, and by the Einstein BIH Fellowship Award to M. N.

C. A. B. and J. J. contributed equally to this work.

[1] B. Alberts, A. Johnson, J. Lewis, D. Morgan, and M. Raff, *Molecular Biology of the Cell* (Garland Science, New York, 2014).
[2] S. Chambeyron and W. A. Bickmore, Curr. Opin. Cell Biol. **16**, 256 (2004).
[3] D. Marenduzzo, C. Micheletti, and P. R. Cook, Biophys. J. **90**, 3712 (2006).
[4] A. Hanke and R. Metzler, Biophys. J. **85**, 167 (2003).
[5] J. M. G. Vilar and L. Saiz, Phys. Rev. Lett. **96**, 238103 (2006).
[6] J. Dekker, K. Rippe, M. Dekker, and N. Kleckner, Science **295**, 1306 (2002).
[7] S. S. P. Rao, M. H. Huntley, N. C. Durand, E. K. Stamenova, I. D. Bochkov, J. T. Robinson, A. L. Sanborn, I. Machol, A. D. Omer, E. S. Lander *et al.*, Cell **159**, 1665 (2014).
[8] J. R. Dixon, S. Selvaraj, F. Yue, A. Kim, Y. Li, Y. Shen, M. Hu, J. S. Liu, and B. Ren, Nature (London) **485**, 376 (2012).
[9] E. de Wit, E. S. M. Vos, S. J. B. Holwerda, C. Valdes-Quezada, M. J. A. M. Verstegen, H. Teunissen, E. Splinter, P. J. Wijchers, P. H. L. Krijger, and W. de Laat, Mol. Cell **60**, 676 (2015).
[10] M. Oti, J. Falck, M. A. Huynen, and H. Zhou, BMC Genomics **17**, 252 (2016).
[11] L. A. Mirny, Chromosome Res. **19**, 37 (2011).
[12] Z. Tang *et al.*, Cell **163**, 1611 (2015).
[13] F. Uhlmann, Nat. Rev. Mol. Cell Biol. **17**, 399 (2016).
[14] P. J. Huis in 't Veld, F. Herzog, R. Ladurner, I. F. Davidson, S. Piric, E. Kreidl, V. Bhaskara, R. Aebersold, and J. M. Peters, Science **346**, 968 (2014).
[15] K. Nasmyth, Nat. Cell Biol. **13**, 1170 (2011).
[16] R. Metzler, A. Hanke, P. G. Dommersnes, Y. Kantor, and M. Kardar, Phys. Rev. E **65**, 061103 (2002).
[17] D. Michieletto, Soft Matter **12**, 9485 (2016).
[18] J. Stigler, G. Çamdere, D. E. Koshland, and E. C. Greene, Cell Rep. **15**, 988 (2016).
[19] M. T. Ocampo-Hafalla and F. Uhlmann, J. Cell Sci. **124**, 685 (2011).
[20] D. Gerlich, B. Koch, F. Dupeux, J. M. Peters, and J. Ellenberg, Curr. Biol. **16**, 1571 (2006).
[21] R. Ladurner, V. Bhaskara, P. J. H. in't Veld, I. F. Davidson, E. Kreidl, G. Petzold, and J. M. Peters, Curr. Biol. **24**, 2228 (2014).
[22] A. S. Hansen, I. Pustova, C. Cattoglio, R. Tjian, and X. Darzacq, eLife **6**, e25776 (2017).
[23] G. A. Busslinger, R. A. Stocsits, P. van der Lelij, E. Axelsson, A. Tedeschi, N. Galjart, and J.-M. Peters, Nature (London) **544**, 503 (2017).
[24] E. Alipor and J. F. Marko, Nucleic Acids Res. **40**, 11202 (2012).
[25] G. Fudenberg, M. Imakaev, C. Lu, A. Goloborodko, N. Abdennur, and L. A. Mirny, Cell Rep. **15**, 2038 (2016).
[26] A. L. Sanborn, S. S. P. Rao, S.-C. Huang, N. C. Durand, M. H. Huntley, A. I. Jewett, I. D. Bochkov, D. Chinnappan, A. Cutkosky, J. Li *et al.*, Proc. Natl. Acad. Sci. U.S.A. **112**, E6456 (2015).
[27] Y. Murayama and F. Uhlmann, Cell **163**, 1628 (2015).
[28] L. Uuskula-Reimand, H. Hou, P. Samavarchi-Tehrani, M. Vietri Rudan, M. Liang, A. Medina-Rivera, H. Mohammed, D. Schmidt, P. Schwalie, E. J. Young *et al.*, Genome Biol. **17**, 182 (2016).
[29] See Supplemental Material at http://link.aps.org/supplemental/10.1103/PhysRevLett.119.138101 for more details on analytical calculations and simulations, and for additional simulation results, supplemental figures and movies. The Supplemental Material also includes Refs. [30–39].
[30] M. R. Evans and S. N. Majumdar, Phys. Rev. Lett. **106**, 160601 (2011).
[31] P. de los Rios and A. Barducci, eLife **3**, e02218 (2014).
[32] S. Plimpton, J. Comput. Phys. **117**, 1 (1995).
[33] J. Langowski, Eur. Phys. J. E **19**, 241 (2006).
[34] K. Kremer and G. S. Grest, J. Chem. Phys. **92**, 5057 (1990).
[35] H. Hajjoul *et al.*, Genome Res. **23**, 1829 (2013).
[36] A. Rosa and R. Everaers, PLoS Comput. Biol. **4**, e1000153 (2008).
[37] A. Rosa, N. B. Becker, and R. Everaers, Biophys. J. **98**, 2410 (2010).
[38] J. Shimada and H. Yamakawa, Macromolecules **17**, 689 (1984).
[39] X. Wang, H. B. Brandao, T. B. K. Le, M. T. Laub, and D. Z. Rudner, Science **355**, 524 (2017).
[40] A. Goloborodko, M. V. Imakaev, J. F. Marko, and L. Mirny, eLife **5**, e14864 (2016).
[41] B. Duplantier, J. Stat. Phys. **54**, 581 (1989).
[42] E. Carlon, E. Orlandini, and A. L. Stella, Phys. Rev. Lett. **88**, 198101 (2002).
[43] C. A. Brackley, J. Johnson, S. Kelly, P. R. Cook, and D. Marenduzzo, Nucleic Acids Res. **44**, 3503 (2016).
[44] M. Barbieri, M. Chotalia, J. Fraser, L.-M. Lavitas, J. Dostie, A. Pombo, and M. Nicodemi, Proc. Natl. Acad. Sci. U.S.A. **109**, 16173 (2012).
[45] C. A. Brackley, S. Taylor, A. Papantonis, P. R. Cook, and D. Marenduzzo, Proc. Natl. Acad. Sci. U.S.A. **110**, E3605 (2013).
[46] A. M. Chiariello, S. Bianco, C. Annunziatella, A. Esposito, and M. Nicodemi, Sci. Rep. **6**, 29775 (2016).
[47] Volume exclusion can though still affect the dynamics, so our theory should not be seen as quantitative.
[48] I. F. Davidson, D. Goetz, M. P. Zaczek, M. I. Molodtsov, P. J. Huis in 't Veld, F. Weissmann, G. Litos, D. A. Cisneros, M. Ocampo-Hafalla, R. Ladurner *et al.*, EMBO J. **35**, 2671 (2016).
[49] M. Kanke, E. Tahara, P. J. Huis in't Veld, and T. Nishiyama, EMBO J. **35**, 2686 (2016).
[50] DOI: 10.7488/ds/2129.